Biomaterials 81 (2016) 14–26

Contents lists available at ScienceDirect

Biomaterials

journal homepage: www.elsevier.com/locate/biomaterials

High-purity magnesium interference screws promote fibrocartilaginous entheses regeneration in the anterior cruciate ligament reconstruction rabbit model via accumulation of BMP-2 and VEGF

Pengfei Cheng [a, 1], Pei Han [a, 1], Changli Zhao [b, **], Shaoxiang Zhang [b, c], Hongliu Wu [b], Jiahua Ni [b], Peng Hou [a], Yuanzhuang Zhang [c], Jingyi Liu [c], Haidong Xu [c], Shen Liu [a], Xiaonong Zhang [b, c, ***], Yufeng Zheng [d], Yimin Chai [a, *]

[a] Orthopaedic Department, Shanghai Jiao Tong University Affiliated Sixth People's Hospital, Shanghai 200233, China
[b] State Key Laboratory of Metal Matrix Composites, School of Materials Science and Engineering, Shanghai Jiao Tong University, Shanghai 200240, China
[c] Suzhou Origin Medical Technology Co. Ltd., Suzhou 215513, China
[d] Department of Materials Science and Engineering, College of Engineering, Peking University, Beijing 100871, China

ARTICLE INFO

Article history:
Received 30 November 2015
Accepted 3 December 2015
Available online 15 December 2015

Keywords:
High-purity magnesium
Interference screw
Anterior cruciate ligament reconstruction
Fibrocartilaginous entheses
BMP-2
VEGF

ABSTRACT

Interference screw in the fixation of autologous tendon graft to the bone tunnel is widely accepted for the reconstruction of anterior cruciate ligament (ACL), but the regeneration of fibrocartilaginous entheses could hardly be achieved with the traditional interference screw. In the present work, biodegradable high-purity magnesium (HP Mg) showed good cytocompatibility and promoted the expression of bone morphogenetic protein-2 (BMP-2) and vascular endothelial growth factor (VEGF), fibrocartilage markers (Aggrecan, COL2A1 and SOX-9), and glycosaminoglycan (GAG) production *in vitro*. The HP Mg screw was applied to fix the semitendinosus autograft to the femoral tunnel in a rabbit model of ACL reconstruction with titanium (Ti) screw as the control. The femur-tendon graft-tibia complex was retrieved at 3, 6, 9 and 12 weeks. Gross observation and range of motion (ROM) of the animal model reached normal levels at 12 weeks. No sign of host reaction was found in the X-ray scanning. The HP Mg group was comparable to the Ti group with respect to biomechanical properties of the reconstructed ACL, and the ultimate load to failure and stiffness increased 12 weeks after surgery. In the histological analysis, the HP Mg group formed distinct fibrocartilage transition zones at the tendon-bone interface 12 weeks after surgery, whereas a disorganized fibrocartilage layer was found in the Ti group. In the immunohistochemical analysis, highly positive staining of BMP-2, VEGF and the specific receptor for BMP-2 (BMPR1A) was shown at the tendon-bone interface of the HP Mg group compared with the Ti group. Furthermore, the HP Mg group had significantly higher expression of BMP-2 and VEGF than the Ti group in the early phase of tendon-bone healing, followed by enhanced expression of fibrocartilage markers and GAG production. Therefore we proposed that the stimulation of BMP-2 and VEGF by Mg ions was responsible for the fibrochondrogenesis of Mg materials. HP Mg was promising as a biodegradable interference screw with the potential to promote fibrocartilaginous entheses regeneration in ACL reconstruction.

1. Introduction

The anterior cruciate ligament (ACL) stabilizes the knee joint in motion and transmits mechanical force to the bone by fibrocartilaginous entheses [1,2]. Fibrocartilaginous entheses consist of four consecutive layers in the sequence from soft to hard tissues: ligament, uncalcified fibrocartilage, calcified fibrocartilage, and

* Corresponding author.
** Corresponding author.
*** Corresponding author. State Key Laboratory of Metal Matrix Composites, School of Materials Science and Engineering, Shanghai Jiao Tong University, Shanghai 200240, China.
E-mail addresses: zcl@sjtu.edu.cn (C. Zhao), xnzhang@originmedtech.com (X. Zhang), chaiyimin@vip.163.com (Y. Chai).
[1] These two authors contributed equally.

http://dx.doi.org/10.1016/j.biomaterials.2015.12.005
0142-9612/

bone. The complicated structure cannot be regenerated after modern sport-related injuries without surgical intervention, [3]. Thus autologous tendon grafts with interference screws in fixation are broadly accepted in ACL reconstruction surgery [4,5]. Non-degradable interference screws made of titanium provide high mechanical strength for tendon graft fixation. Unfortunately, these screws may impair the tendon graft during screw insertion or aggressive rehabilitation [6] and require secondary surgery for removal [7]. Interference screws made of biodegradable polymers, such as poly-L-lactide, are put into wide application because they can gradually be replaced by the patient's own tissue. However, the biodegradable interference screws often crack during screw insertion due to inadequate mechanical strength [8,9]. Additionally, adverse reactions such as synovitis, granuloma and tunnel enlargement have been reported in their degradation process [10,11]. Furthermore, the healing of tendon grafts fixed by the current interference screws is poor, with fibrous scar tissue layer formation at the tendon-bone interface. The fibrous layer was relatively weak compared to the native fibrocartilaginous entheses and greatly impaired joint stability during aggressive rehabilitation [12,13]. Therefore, new materials for interference screw with the potential to promote fibrocartilaginous entheses regeneration are desired in ACL reconstruction surgery.

Recently, magnesium has been investigated as a potential biomaterial for biodegradable orthopedic implants. Magnesium possesses good biocompatibility and mechanical properties that could meet the load requirement in the knee joint during implantation and aggressive rehabilitation [14,15]. Furthermore, Mg could benefit the ACL reconstruction because it was reported to stimulate fibrocartilaginous entheses regeneration. Hagandora et al. [16] cultured isolated goat costal fibrochondrocytes in medium with different concentrations of Mg ions, and showed a high increase in production of fibrocartilage matrix (Collagen II and glycosaminoglycan (GAG)) when the Mg ion concentration increased up to 20 mM. Feyerabend et al. [17] and Dou et al. [18] showed that the nonphysiologically high Mg concentration resulted in an increase of GAG production during the re-differentiation of chondrocytes. However, few articles reported the influence of Mg interference screw on the fibrocartilaginous entheses regeneration within the ACL reconstruction animal model.

Growth factors are critical to induce tissue regeneration at the tendon-to-bone interface [19]. The most widely investigated growth factors are the bone morphogenetic proteins (BMP) [20]. Recombinant BMPs effectively induce new tendon, cartilage, ligament, and bone formation in both clinical and animal studies [21,22]. Angiogenesis is important for tendon-bone healing, and vascular endothelium growth factor (VEGF) can contribute to blood vessel ingrowth at the fibrocartilage zone between the tendon graft and the bone tunnel [23]. Related researches have confirmed that Mg ions could promote the expression of BMP-2 and VEGF in isolated pluripotent stem cells and bone defect animal model [24,25]. Therefore, it is necessary to experimentally determine whether the Mg devices influence growth factors in ACL reconstruction and promote fibrocartilaginous entheses regeneration.

Therefore, in the present study, high-purity magnesium (HP Mg) screws were applied to the rabbit model of ACL reconstruction with titanium (Ti) screws as the control. The influence of HP Mg on fibrocartilaginous entheses regeneration was evaluated both *in vitro* and *in vivo*, and the relationship between HP Mg and growth factors (BMP-2 and VEGF) was investigated to elucidate the mechanism of Mg ions promoting fibrocartilaginous entheses regeneration.

2. Materials and methods

2.1. Materials preparation

The HP Mg (99.98 wt%) screws and biomedical Ti (TA1ELI, 99.8 wt%) screws were supplied by Suzhou Origin Medical Technology Co. Ltd., China. The screws were designed according to rabbit knee joint geometry, with a total length of 12 mm, shaft outer diameter of 2.7 mm and shaft inner diameter of 2.1 mm (Fig. 1a). All samples were rinsed in acetone and ethanol successively, washed in distilled water, and then sterilized with 29 kGy of ^{60}Co radiation.

2.2. In vitro cell experiment

2.2.1. Preparation of biomaterial extracts

Screw extracts were prepared according to the methods described by the International Organization for Standardization (ISO 10993-5). Briefly, HP Mg and Ti screws were immersed in alpha modified Eagle's medium (α-MEM, Hyclone, Logan, USA) supplemented with 10% (v/v) fetal bovine serum (FBS, Invitrogen, Carlsbad, USA), 100 U/ml penicillin and 100 mg/ml streptomycin at 37 °C in a humidified atmosphere of 5% CO_2 for 24 h. The ratio of screw samples to culture medium was 0.2 g/mL. The Mg ion concentration and pH value of the HP Mg extracts were measured by inductively coupled plasma atomic emission spectroscopy (ICP-AES, VISTAPRO, Agilent, USA) and a pH meter (PB-10, Sartorius, Germany), respectively.

2.2.2. Cell viability

The MTT assay was conducted to evaluate cell viability of human bone marrow-derived mesenchymal stem cells (hBMSCs) cultured in the extracts. hBMSCs were collected according to the reported method [26], and the protocol was approved by the Ethics Committee of Shanghai Jiao Tong University Affiliated Sixth People's Hospital. Cells (7×10^4 cells/100 μl) were seeded in 96-well plates with α-MEM culture medium and were placed in a humidified incubator containing 5% CO_2 at 37 °C. After 24 h of incubation, cells were treated with HP Mg or Ti extracts for 1, 3 and 5 days, respectively. Twenty microlitres of the MTT solution and 80 μl of α-MEM culture medium were added to each well and were further incubated for 4 h. Then, 100 μl of dimethylsulfoxide was added to each well and incubated for a further 0.5 h. Finally, the absorbance was recorded by a multimode detector on a Beckman Coulter DTX 880 (Beckman Coulter, Brea, USA) at a wavelength of 490 nm. Cell viability was determined from the absorbance readings.

2.2.3. Real-time quantitative polymerase chain reaction (RT-qPCR) analysis

Gene expression of fibrocartilage markers (Aggrecan, COL2A1 and SOX-9) [27], BMP-2 and VEGF was determined by RT-qPCR after 1, 7 and 14 day cultures. Briefly, total RNA of hBMSCs in the HP Mg extracts, Ti extracts and α-MEM culture medium (control group) was isolated using TRIZOL reagent (Invitrogen, Carlsbad, USA). Isolated RNA was reverse-transcribed into cDNA using the SuperScript III First-Strand Synthesis System (Invitrogen, Carlsbad, CA), and the cDNA product was amplified with recombinant Platinum Taq DNA polymerase (Invitrogen). A Bio-Rad C1000 was used for the RT-qPCR analysis with SYBR Premix Ex Taq II (Takiron, Osaka, Japan). The primer sequences for the hBMSCs are listed in Table 1. The expression was evaluated and normalized to the internal standard gene (18s).

2.2.4. Glycosaminoglycan (GAG) assay

The total sulphated GAG concentration of hBMSCs was

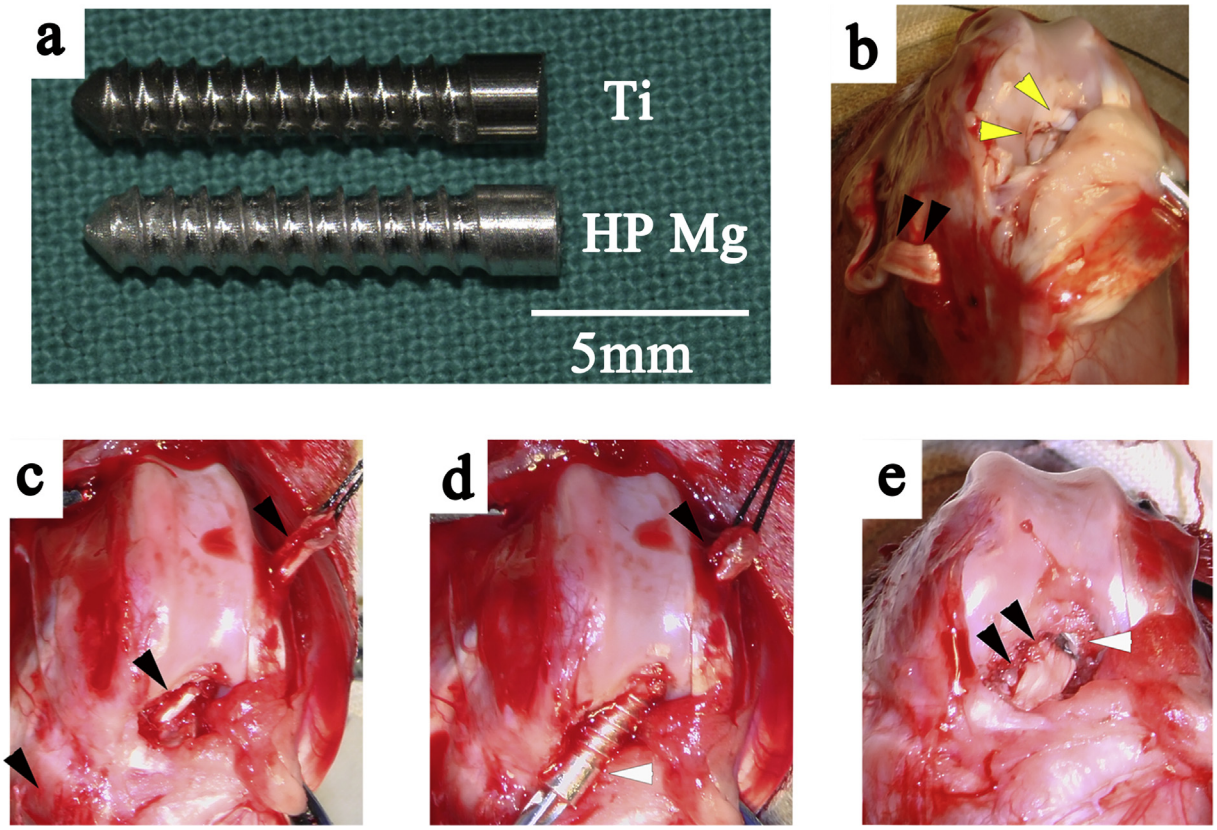

Fig. 1. (a) Ti (upper) and HP Mg (lower) screws. The critical surgery procedure in the ACL reconstruction involved (b) transection of the native ACL (yellow arrowheads) and harvest of the semitendinosus (black arrowheads); (c) semitendinosus through the femoral and tibial tunnels; (d) insertion of an HP Mg screw (white arrowheads) into the femoral tunnel; (e) semitendinosus fixed to the femoral tunnel by an HP Mg screw (white arrowheads). (For interpretation of the references to colour in this figure legend, the reader is referred to the web version of this article.)

Table 1
Primer pairs for the hBMSCs used in the RT-qPCR analysis.

Gene	Forward primer	Reverse primer
SOX-9	5-CCCTTCAACCTCCCACACTAC-3	5-TCCTCAAGGTCGAGTGAGCTG -3
COL2A1	5-GCTCCCAGAACATCACCTACC-3	5-TGAACCTGCTATTG CCCTCT-3
Aggrecan	5-GGCTGCTGTCCCCGTAGAAGA-3	5-GGGAGGCCAAGTAGGAAGGAT-3
VEGF	5-ACCTCATGCTGATACCGGGTCC-3	5-CCGGGGCGTGGAG-TACCTGT-3
BMP-2	5-AAGCCAAACACAAACAGCGG-3	5-TTCTCCGTGGCAGTAAAAGGC -3
18s	5-GTTCTTAGTTGGTGGAGCGATTT-3	5-CGGACATCTAAGGGCATCACA-3

quantified using a Blyscan Kit (Biocolor Ltd, Ireland) [28]. hBMSCs were treated with HP Mg extracts, Ti extracts and α-MEM culture medium (control group) for 1, 7 and 14 days. Then, the hBMSCs were washed twice with cold phosphate-buffered saline (PBS). After repeated freezing and thawing, cells were combined with 1,9-dimethylmethylene blue (DMMB) dye. The concentration of the GAG-DMMB complexes was determined using a plate reader at 540 and 595 nm and was correlated to a standard prepared with chondroitin-6-sulfate. The corresponding DNA concentration was determined using the PicoGreen dsDNA assay (Molecular Probes) following the protocol suggested by the manufacturer. The relative GAG content was expressed as μg GAG/μg DNA in the corresponding tissues.

2.3. Preliminary animal study

2.3.1. Rabbit model of ACL reconstruction

The experimental protocol was approved by the Animal Care and Experiment Committee of Shanghai Jiao Tong University Affiliated Sixth People's Hospital. Sixty skeletally mature, male, New Zealand white rabbits were used as the ACL reconstruction model. Briefly, under general anaesthesia, medial parapatella arthrotomy was performed on the right leg to expose the knee joint. Native ACL was completely transected, and gross anterior subluxation of patella was done manually. The proximal end of the semitendinosus was freed (Fig. 1b). With the knee positioned in 45° flexion, a bone tunnel of 2.1 mm in diameter was created from the medial side of the tibia to the lateral-anterior femoral condyle. The semitendinosus was pulled through both the femoral and tibial tunnel using an 18-gauge needle (Fig. 1c). Under graft tensioning, the screw was implanted into the femoral tunnel after countersinking by drill bit (Fig. 1d). The distal end of the semitendinosus was sutured to the neighbouring periosteum (Fig. 1e). The wound was irrigated with povidone iodine solution. Then the skin and fascia were closed in layers.

Following surgery, rabbits were housed in separate cages and were allowed to eat and drink ad libitum after anabiosis. Antibiotic (amoxicillin 150 mg/10 kg weight) was administered

subcutaneously for the following 3 days. Signs of limping, joint swelling, subcutaneous emphysema and loss of appetite were recorded daily before sacrifice.

2.3.2. X-ray scanning

At 3, 6, 9 and 12 weeks after surgery, X-ray scanning of the rabbit knee joint in the anterior–posterior position was performed. The operation conditions of the X-ray machine (Digital Diagnost, Philips, Amsterdam, Netherlands) were set as follows: 52 kV, 3.2 mA s and 10.9 ms. The X-ray radiographs reflected the host reaction in the knee joint with respect to soft tissue swelling, osteolysis, deformity and joint dislocation.

2.3.3. Gross observation

The macroscopic evaluation of knee joint at 3, 6, 9 and 12 weeks after ACL reconstruction was performed according to the adjusted Oswestry Arthroscopy Score (OAS) macroscopic assessment (Table 2) [29]. Three independent observers who were blinded to the experimental groups performed the evaluation, and the average value was calculated.

2.3.4. Range of motion (ROM) of knee joint

The ROM of knee joint was measured with the rabbits under anesthesia using a goniometer. In Brief, the point at proximal femur, distal tibia, and lateral femoral condyle were localized by goniometer to measure the knee joint angle, and the average value of three measurements per rabbit was calculated.

2.3.5. Biomechanical tests

Biomechanical tests were conducted on the femur-tendon graft-tibia complexes immediately after surgery (0 week) and at 12 weeks post-surgery. At 3, 6, 9 and 12 weeks, the femur-tendon graft–tibia complexes were harvested at 60 mm in the femur and 60 mm in the tibia immediately after sacrifice. All soft tissue was removed by sharp dissection, except the reconstructed ACL. A Zwick materials testing machine (Z020, Zwick/Roell, Germany) was used to assess the biomechanical properties of reconstructed ACL. Each sample was aligned parallel to the axis of the applied loads with a preloading of 1 N and a load displacement rate at 0.5 mm/min. The failure modes of the tendon graft, ultimate load to failure (N) and related stiffness (N/mm) were recorded according to the reference [30].

2.3.6. Micro-computed tomography (micro-CT) scanning

Micro-CT scanning was conducted using a laboratory Micro-CT Scanner eXplore RS 80 (GE Healthcare, Little Chalfont, UK). The X-ray tube was set at 80 kV and 450 μA with a scan resolution of 45 μm and an exposure time of 400 ms. The volume of the HP Mg screw was measured using Micro View 2.2 Advanced Bone Analysis Application software (GE Health Systems, Waukesha, WI, USA) in accordance with a previous report [31].

2.3.7. Histological and immunohistochemical analysis

Femur-tendon graft-tibia complexes were fixed in 4% neutral-buffered formalin for 48 h. Then, the samples were decalcified in 9% formic acid for 9 weeks at room temperature. The samples were dehydrated by graded ethanol and were embedded in paraffin. The samples were cut into 4-μm slices. Consecutive sections were stained with haematoxylin-eosin (HE), Mallory, Toluidine blue and Safranin O/fast green. The tendon-bone interface was graded by three trained observers according to one modified histological score system for tendon-bone healing in ACL reconstruction (Table 3) [32]. The relative area of fibrocartilage at the tendon-bone interface was calculated using an image analyser (Image-Pro Plus, Media Cyberbetics, USA) according to previous studies [33,34].

Expression of BMP-2, VEGF and the specific receptor for BMP-2 (BMPR1A) at the tendon-bone interface was analysed by immunohistochemical staining. The sections were dewaxed in xylene and then hydrated through graded alcohols. The endogenous peroxidase activity was quenched in 0.3% hydrogen peroxide for 10 min. After blocking with 1% goat serum (1:100 dilution, Sigma), sections were incubated with primary antibodies against BMP-2 (Abcam, Cambridge, UK), VEGF (Abcam, Cambridge, UK) and BMPR1A (Abcam, Cambridge, UK) overnight at 4 °C. After washing with PBS for 3 times, sections were incubated in secondary antibody for 1 h at 37 °C. Staining was developed in 3,3'-diaminobenzidine (DAB) solution (Dako, Hamburg, Germany) with haematoxylin counterstaining. The immunohistochemical sections were scored using a 5-grade scoring system (Table 4), which was adopted from Lovric et al. [35].

2.3.8. Western blot analysis

At 3, 6, 9 and 12 weeks after surgery, tissues at the insertion site of the interference screw were collected and immediately frozen, with native ACL entheses on the left leg as the control. For the western blot assay, the tissues were homogenized in 200 μl of ice-cold RIPA (Bio-Rad, Hercules, USA) supplemented with complete protease inhibitor. After incubation on ice for 30 min and centrifugation at 12,000 rpm for 10 min, the supernatant fluid was collected. The total protein content was measured by the BCA protein assay kit (Thermo, Rockford, USA) and was then adjusted to 10 μg/μL. Ten microliters of supernatant fluid was loaded onto a 10%

Table 2
Macroscopic evaluation of ACL reconstruction.

Item	Description	Score
Level at insertion site with surrounding cartilage	Level	2
	Raised	1
	Below	0
Integration at the insertion site with surrounding tissue	Complete	2
	Minor disruption (<25% of area)	1
	Major disruption (>25% of area)	0
Stiffness of tendon graft	Normal compared to posterior cruciate ligament	2
	Softer	1
	Very soft/hard	0
Appearance of articular surface	Smooth	2
	Fine fronds	1
	Severe fronds	0
Colour of articular surface	Pearly, hyaline-like	2
	Gloomy white	1
	Yellow bone	0
Total		10

Table 3
Histological evaluation of the tendon graft to bone tunnel healing in ACL reconstruction.

Item	Description	Score
Tendon graft bonding to adjacent tissue	Slight (0%–25% of tendon-bone interface)	0
	Moderate (25%–50% in tendon-bone interface)	1
	Substantial (50%–75% in tendon-bone interface)	2
	Intense (75%–100% in tendon-bone interface)	3
Fibrocartilage formation	None (0% in tendon-bone interface)	0
	Slight (0%–30% in tendon-bone interface)	1
	Moderate (30%–60% in tendon-bone interface)	2
	Abundant (60%–100% in tendon-bone interface)	3
Calcification accumulation	None (0% in tendon-bone interface)	0
	Slight (<30% in tendon-bone interface)	1
	Moderate (<60% in tendon-bone interface)	2
	Abundant (≥75% in of tendon-bone interface)	3
Total		9

Table 4
Immunohistochemical evaluation of growth factors at the tendon-bone interface of the ACL reconstruction.

Items		Score
Percentage of positively stained cells versus whole cell population	Staining intensity	
0%	No	0
<10%	Weak	1
<25%	Strong	2
<50%	Moderate	2
<50%	Strong	3
<80%	Moderate	3
>80%	Strong	4

SDS-PAGE gel and then transferred onto a polyvinylidenefluoride (PVDF) membrane (Millipore, Billerica, MA). After blocking with 5% skim milk, the membranes were incubated overnight at 4 °C with primary antibodies against BMP-2 (Abcam, Cambridge, UK), VEGF (Abcam, Cambridge, UK) and GAPDH (Cell Signaling, Danvers, MA), respectively. After washing with TBST buffer (50 mm Tris—HCl, 100 mm NaCl, and 0.1% Tween-20, pH 7.4), the membranes were incubated with the secondary antibody (Cell Signaling, Beverly, MA) for 1 h. Then, the membranes were scanned with an imaging system (Image Quant LAS 4000 mini, GE), and the densitometry of the bands was analysed with Image Pro-plus 6.0 (Media Cybernetics, USA).

2.3.9. *In vivo fibrochondrogenesis induction assessment*

Tissues surrounding the tendon-bone interface at 3, 6, 9 and 12 weeks were collected for RT-qPCR and GAG assay. The sample analysis by RT-qPCR and western blotting was performed as follows. For RT-qPCR analysis, the RNA was extracted using TRIZOL reagent and a tissue homogenizer (Bead Ruptor 12, Omni, USA). The primer sequences for rabbit samples are listed in Table 5. For the GAG assay, tissues after drying treatment were weighed, and the total GAG was extracted with Papain Extraction Reagent (Sigma—Aldrich, St. Louis, USA) using the Blyscan Kit. The GAG content within the test samples was expressed as μg GAG/mg tissues.

2.4. *Statistical analysis*

All experiments were conducted in triplicate, and the data were presented as the means ± standard deviation. Statistical analysis was performed with SPSS 17.0 (SPSS Inc., Chicago, USA). One-way ANOVA and the Student-Newman-Keuls post hoc test determined the level of significance in the differences between groups. P values less than 0.05 and 0.01 were considered to be significant and highly significant, respectively.

3. Results

3.1. *In vitro cell viability*

The concentration of Mg ions in HP Mg extracts was 4.16 ± 0.21 mM, and the pH was 7.93 ± 0.16. HP Mg extracts were confirmed to stimulate cell viability, with 156.6 ± 6.9% at 1 day, 163.3 ± 13.7% at 3 days and 197.9 ± 21.6% at 5 days. In comparison, the cell viability of the Ti group was similar to the normal culture medium at 1, 3 and 5 days (Fig. 2a).

3.2. *In vitro expression of growth factors and fibrocartilage markers*

Fig. 2b shows that the expression of BMP-2 and VEGF was significantly higher in the HP Mg group than in other groups at 7 and 14 days ($p < 0.01$), suggesting that the HP Mg extracts were more effective in stimulating BMP-2 and VEGF expression than Ti extracts.

The expression of fibrocartilage markers (Aggrecan, COL2A1 and SOX-9) is shown in Fig. 2b. There was no significant difference in the expression of Aggrecan among the HP Mg group, Ti group and control group at 1 day and 7 days. However, at 14 days, the HP Mg group showed a dramatic increase in Aggrecan expression, whereas the Ti group and control group maintained their original levels. The changing trends of COL2A1 and SOX-9 were similar to that of Aggrecan. In the HP Mg extracts, the BMP-2 and VEGF expression of hBMSCs increased at 7 days, whereas the expression of fibrocartilage markers did not increase until 14 days, suggesting that the accumulation of BMP-2 and VEGF plays an essential role in fibrochondrogenesis promoted by HP Mg extracts.

3.3. *In vitro GAG production*

The GAG assay reflected the influence of the HP Mg extracts on the fibrocartilage matrix production. As shown in Fig. 2c, the GAG production in the HP Mg group obviously increased at 14 days, which was significantly higher than that in the other groups. In contrast, no significant difference was detected between the Ti group and the control group throughout the experimental period. The results indicated that the HP Mg extracts effectively promoted the production of the fibrocartilage matrix.

3.4. *In vivo animal study of fibrocartilaginous entheses*

All rabbits resumed normal ambulation and daily activity 12 weeks after surgery. No signs of infection, subcutaneous emphysema, wound split or loss of appetite were detected.

3.4.1. *X-ray scanning*

Host reaction to the screws was evaluated by X-ray scanning (Fig. 3). Soft tissue swelling around the knee was found in the HP Mg group at 3 weeks. At 6 weeks, the swelling vanished, and slight periosteal reaction occurred. In the Ti group, swelling of the knee joint was observed within 6 weeks postoperatively, but the periosteal reaction was not observed. Throughout the experimental period, the HP Mg screws demonstrated good biocompatibility, with no signs of osteolysis, deformity or dislocation.

3.4.2. *Gross observation*

Macroscopic observations of the reconstructed ACL are shown in Fig. 4a. At 3 weeks, the insertion site of the tendon graft was directly exposed and caused obvious disruption of the surrounding cartilage. At 6 weeks, the insertion site was covered with synovial

Table 5
Primer pairs for the rabbit samples used in the RT-qPCR analysis.

Gene	Forward primer	Reverse primer
SOX-9	5-ACCAGAACTCGGGGTCCTACT-3	5-TAGGTGAAGGTGGAGTAGAGGCT-3
COL2A1	5-TGAAGACACCAAGGACTGCC-3	5-GCAGTGGCGAGGTCAGTAG-3
Aggrecan	5-CATCTGGAGTTCTTTTTGGGAG-3	5-CAGGTCAGGGATTCTGTGTGTC-3
GAPDH	5-CCGCCCAGAACATCATCCCT-3	5-GCACTGTTGAAGTCGCAGGAGA-3

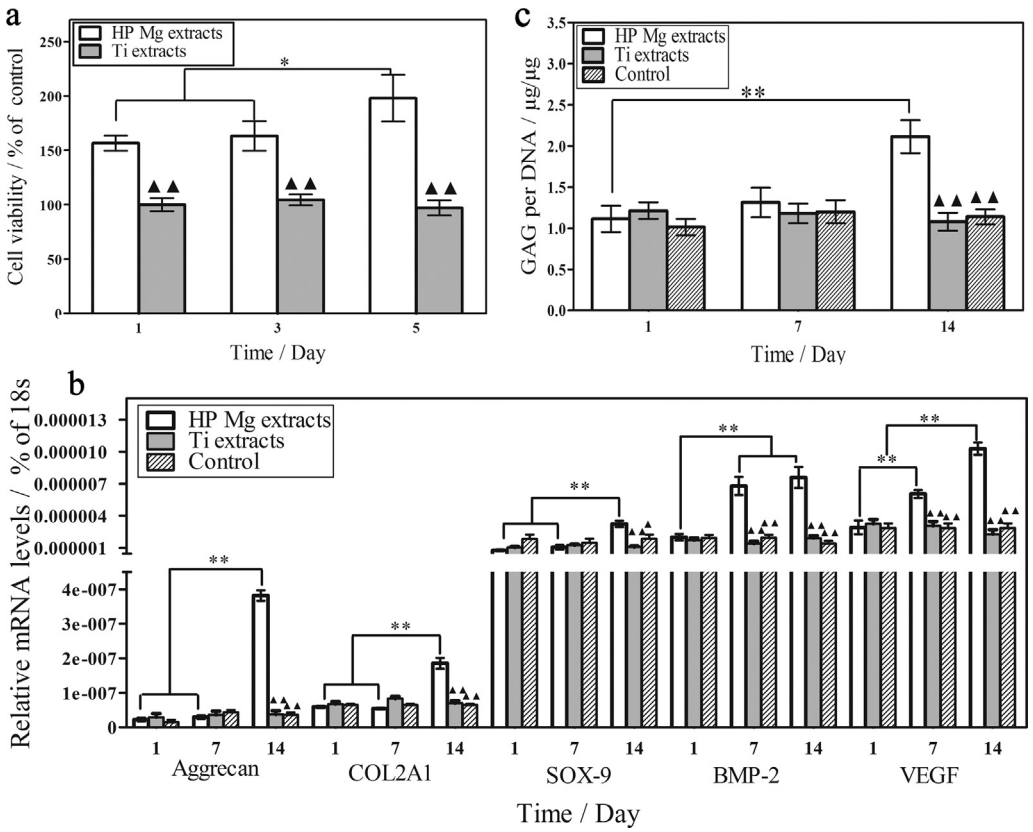

Fig. 2. (a) Cell viability of hBMSCs after culturing in HP Mg extracts and Ti extracts for 1,3 and 5 days. (b) Gene expression of the fibrocartilage markers (Aggrecan, COL2A1, SOX-9), BMP-2 and VEGF of hBMSCs and (c) GAG production of hBMSCs after culturing in HP Mg extracts, Ti extracts and α-MEM culture medium (control group) for 1, 7 and 14 days. * denotes $p < 0.05$; ** denotes $p < 0.01$; ▲ denotes $p < 0.05$ compared with the HP Mg extract group; ▲▲ denotes $p < 0.01$ compared with the HP Mg extract group.

membrane-like tissues. Complete integration with the surrounding cartilage was observed at 9 and 12 weeks. The articular surface remained in good condition throughout the experimental period. The HP Mg and Ti groups showed no significant differences in macroscopic scores, and the reconstructed ACL was comparable to native ACL in morphology at 12 weeks (Fig. 4b).

3.4.3. ROM tests

ROM reflected the functional recovery of the knee joint. As shown in Fig. 4c, ROM in both groups gradually increased with time, and the ROM in the HP Mg group was at the same level as that in the Ti group. At 9 weeks, the ROM in the HP Mg group increased to 147.0 ± 11.4°, a significantly higher value than at 3 weeks ($P < 0.01$). Simultaneously, the ROM in the Ti group increased to 136.0 ± 10.8°. At 12 weeks, the ROM reached 155.0 ± 10.5° and 153.0 ± 12.5° in the HP Mg group and the Ti group, respectively, close to the normal value.

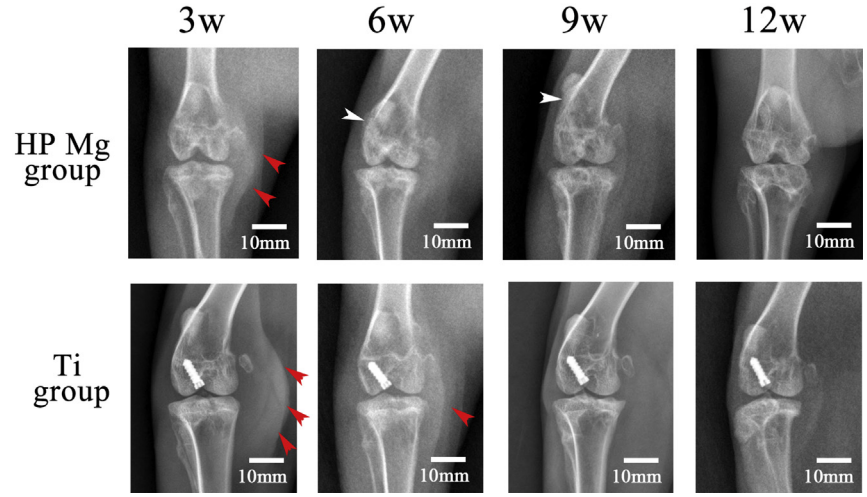

Fig. 3. X-ray images of the rabbit knee joint in the anterior–posterior position at 3, 6, 9 and 12 weeks post-operation (red and white arrowheads indicate soft tissue swelling and periosteal reaction, respectively). (For interpretation of the references to colour in this figure legend, the reader is referred to the web version of this article.)

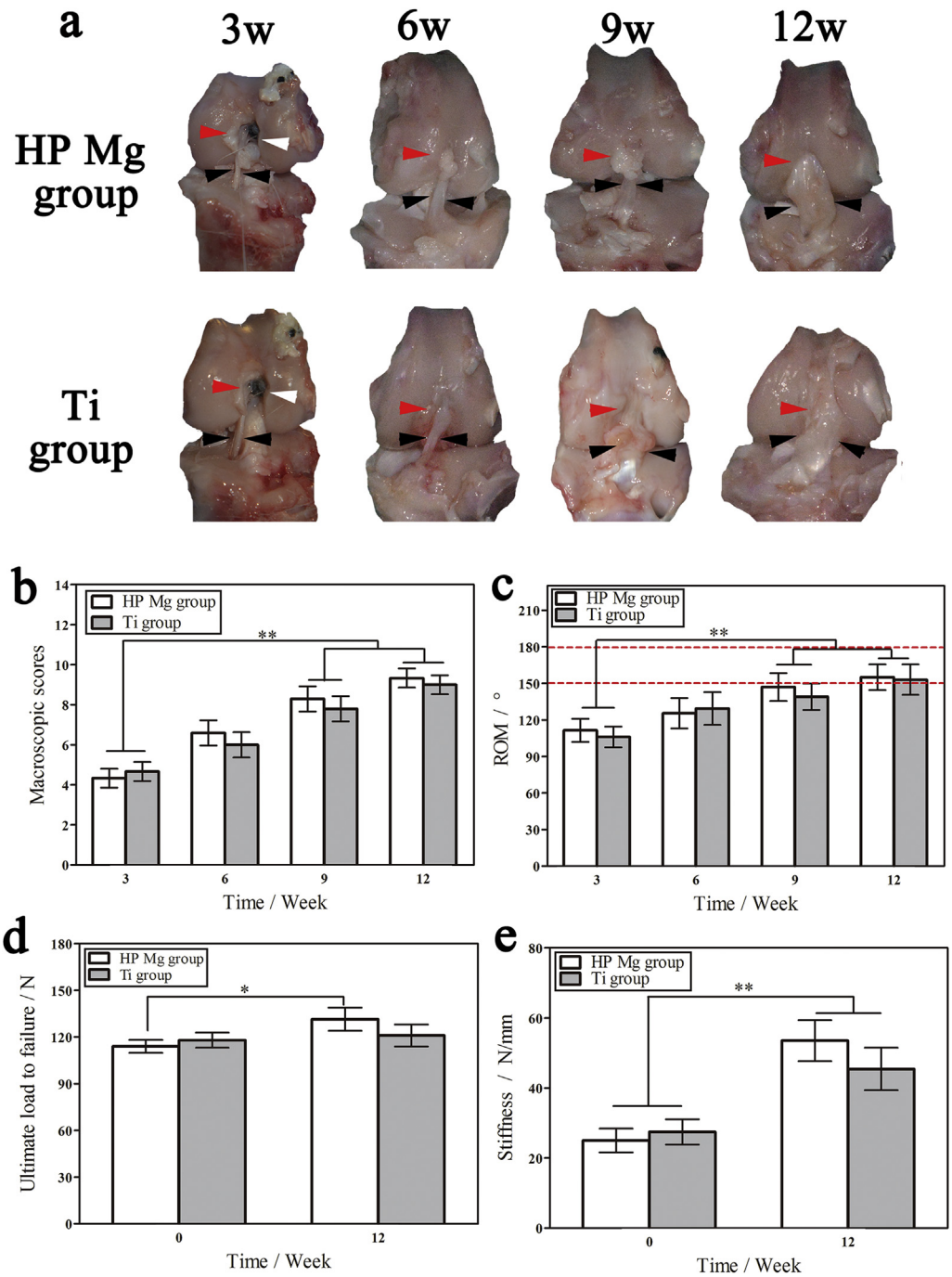

Fig. 4. (a) Macroscopic observation of the rabbit knee joint 3, 6, 9 and 12 weeks after surgery. The tendon graft (black arrowhead) was fixed to the femoral tunnel at the insertion site (red arrowhead) of interference screws (white arrowhead). (b) Macroscopic scores for tendon-bone healing in ACL reconstruction. (c) Maximum ROM of the knee joint (the red dashed line shows the normal range of knee ROM between 150° and 180°). (d) Ultimate load to failure at 0 week and 12 weeks after surgery. (e) Stiffness at failure at 0 week and 12 weeks after surgery. * denotes $p < 0.05$; ** denotes $p < 0.01$. (For interpretation of the references to colour in this figure legend, the reader is referred to the web version of this article.)

3.4.4. Biomechanical analysis

Fig. 4d and e shows the ultimate load to failure and related stiffness of the reconstructed ACL. At 0 week, both the ultimate load to failure and stiffness in the HP Mg group showed no significant difference compared with that in the Ti group, reflecting that the initial mechanical strength of the tendon graft fixed by the HP Mg screw was comparable to that of the Ti screw. At 12 weeks, both the HP Mg group and Ti group showed a large increase in the ultimate load to failure and stiffness ($P < 0.01$) due to the change in failure mode. All of the tendon grafts were directly pulled out from the femoral tunnel at 0 week. The failure mode changed to fibrocartilaginous avulsion at the femoral insertion site at 12 weeks. The average value of the ultimate load to failure and stiffness in the HP Mg group remained at the same level as in the Ti group despite the corrosion of the HP Mg screw. Thus the HP Mg screw could provide rigid fixation of tendon graft in the process of tendon-bone healing.

3.4.5. Micro-CT assessment

Representative 2D micro-CT images showed that the HP Mg and Ti screws remained at the deployed position, and no bone tunnel enlargement or screw slip was observed throughout the experiment (Fig. 5a). The Ti screw maintained the original morphology within 12 weeks, whereas HP Mg screw suffered obvious corrosion. 3D micro-CT images of the HP Mg screw showed mineral deposition on the surface of screw at 12 weeks, which indicated the balance between screw corrosion and bony incorporation (Fig. 5b). The calculated volume loss of the HP Mg screw was stable, and screw volume decreased from 57.41 ± 0.03 mm^3 at 0 week to 55.17 ± 1.38 mm^3, 53.17 ± 1.93 mm^3, 47.04 ± 2.41 mm^3 and 41.93 ± 3.63 mm^3 at 3, 6, 9 and 12 weeks, respectively (Fig. 5c).

3.4.6. Histological analysis at the tendon-bone interface

Fig. 6a shows the regeneration of the fibrocartilage tissues at the tendon-bone interface. In the early phase of ACL reconstruction, the HP Mg and Ti groups showed a normal crimp pattern in complete discontinuity at the tendon-bone interface at 3 weeks. Graft remodelling in both groups occurred at 6 weeks, and high levels of cellularity and vascularity were observed at the interface.

At 9 weeks, an organized fibrocartilage layer was observed in the HP Mg group. At the tendon-bone interface, the HP Mg group had a fibrocartilage interlayer between the tendon graft and bone tunnel, and fibrochondrocytes at the tendon-bone interface were positively stained by Toluidine blue. In contrast, the fibrocartilage zone in the Ti group blended with fibrovascular tissues without a clear boundary. Based on the semi-quantitative scores, the tendon-bone healing was relatively better in the HP Mg group than in the Ti group ($P < 0.01$) (Fig. 6b). The relative area of fibrocartilage at the interface increased to 34.3 ± 4.9% in the HP Mg group but only to 23.0 ± 3.8% in the Ti group (Fig. 6c).

At 12 weeks, the tendon-bone interface in the HP Mg group was further differentiated into four distinct layers: tendon graft, uncalcified fibrocartilage, calcified fibrocartilage and bone. The highly differentiated fibrocartilage tissue was positively stained by both Safranin O/fast green and Toluidine blue, which indicated that the HP Mg screw promoted the regeneration of fibrocartilage transition zones and fibrocartilaginous entheses. In contrast, the Ti group exhibited less organized fibrocartilage tissue with a relatively small area in the interface. The semi-quantitative scores of the HP Mg group increased to 7.0 ± 0.67 (Fig. 6b), and the relative area of fibrocartilage tissues made up 59.7 ± 5.4% of the interface area (Fig. 6c), which was significantly higher than the Ti group.

3.4.7. Immunohistochemical analysis of BMP-2, VEGF and BMPR1A at the tendon-bone interface

To investigate the distribution and expression of growth factors at the tendon-bone interface, consecutive sections were conducted with immunohistochemical staining of BMP-2, VEGF and BMPR1A (Fig. 6a). BMP-2 stained positive within osteoblasts, osteoprogenitor cells and some fibroblasts. At 3 weeks and 6 weeks postoperatively, both the HP Mg and Ti groups showed highly positive staining of BMP-2 at the tendon-bone interface and the HP Mg group had higher expression of BMP-2 than the Ti group, as shown in Fig. 6d and e. The positive staining of BMP-2 in the surrounding fibrocartilage tissues largely subsided at 9 and 12 weeks. At 12 weeks, the expression of BMP-2 in the surrounding fibrocartilage tissues was weak, and no significant difference was observed between the HP Mg and Ti group.

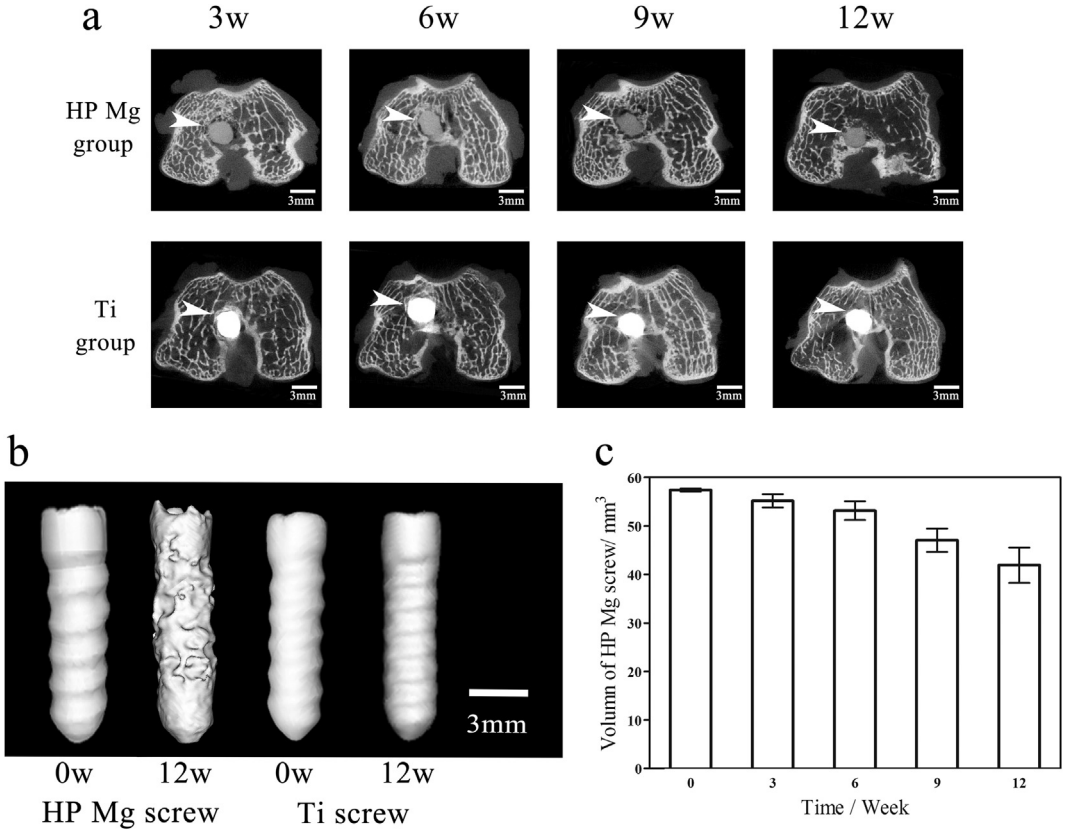

Fig. 5. (a) Representative 2D micro-CT images of the rabbit femur with interference screws (white arrowhead) at 3, 6, 9 and 12 weeks postoperatively. (b) Volume change of the HP Mg screw. (c) 3D micro-CT images of the HP Mg screw *in vivo*.

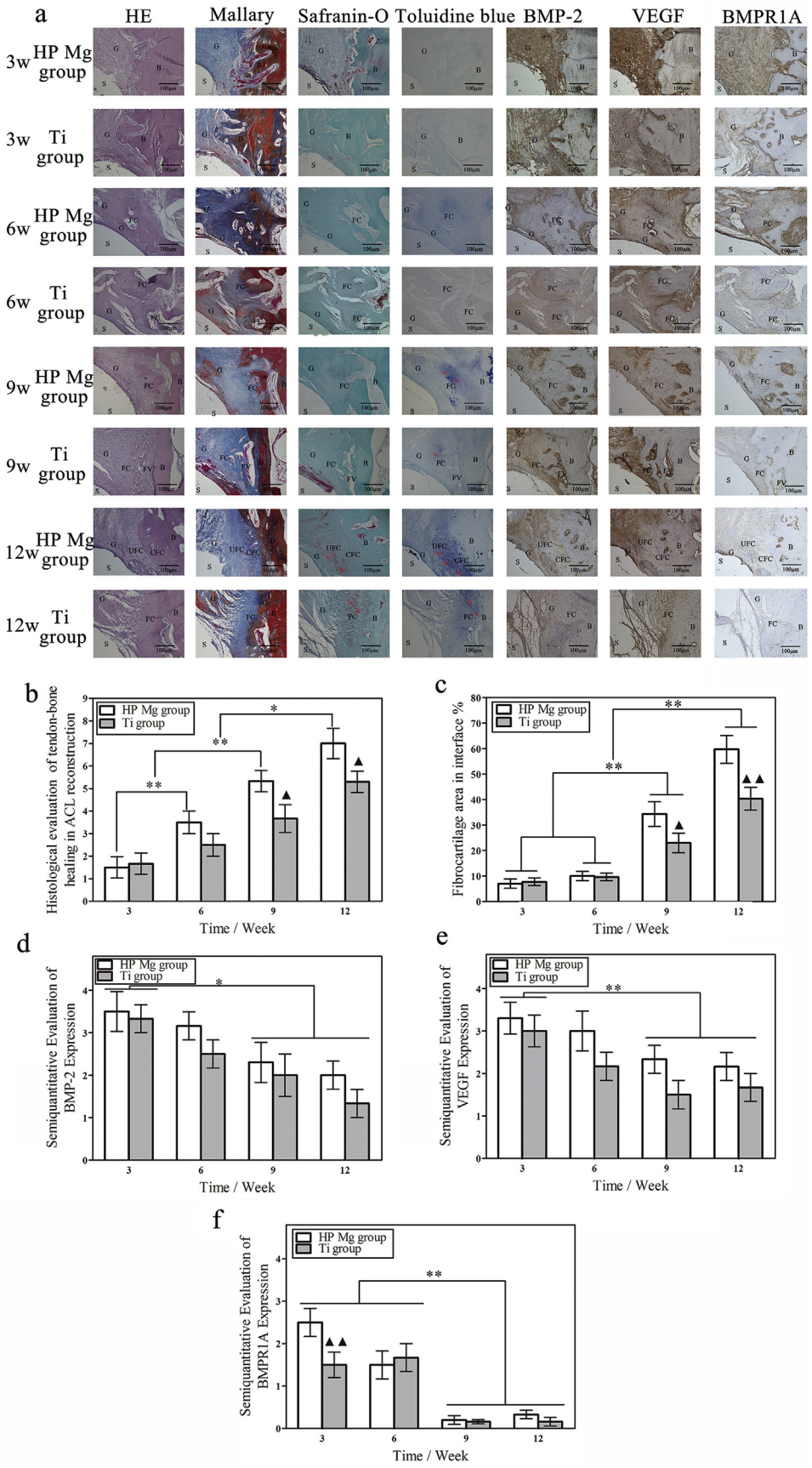

Fig. 6. Histological and immunohistochemical analysis of the tendon-bone interface 3, 6, 9 and 12 weeks after surgery. (a) Representative HE, Mallory, Safranin O/fast green and Toluidine blue stained sections and sections using BMP-2 and VEGF staining. (S represents screw, G represents tendon graft, B represents bone, FV represents fibrovascular tissue, FC

VEGF stained positive within osteoblasts, endothelial cells and some fibroblasts. Positive staining of VEGF was mainly distributed in the tendon tissues rather than bone tissues. The expression of VEGF also decreased with time, which was similar to BMP-2.

BMPR1A was the specific receptor for BMP-2 and the presence of BMPR1A at tendon-bone interface could reflect the activity of related growth factors in ACL regeneration. The distribution and expression of BMPR1A at tendon-bone interface was in consistence with BMP-2. BMPR1A expression also showed the trend of decrease with time and was relatively higher in HP Mg group in simultaneous comparison. It indicated that BMP-2 and VEGF expression was activated in the early phase of tendon-bone healing and the HP Mg screw could promote the activities of BMP-2 and VEGF at the tendon-bone interface.

3.4.8. Western blot analysis of growth factors at the tendon-bone interface

The expression of BMP-2 and VEGF at the tendon-bone interface was quantified by western blot assay (Fig. 7a). During the experimental period, both the HP Mg and Ti groups showed higher expression of BMP-2 and VEGF than the control group (Fig. 7b and c). In both groups, the expression of BMP-2 and VEGF peaked at 3 weeks and then decreased with time, which indicated that BMP-2 and VEGF accumulated in the early phase of the ACL reconstruction process and then gradually decreased with the maturation of the tendon-bone interface. Furthermore, the HP Mg group showed significantly higher expression of BMP-2 and VEGF than the Ti group throughout the experiment. Consistent with the immunohistochemical analysis and *in vitro* RT-qPCR result, the HP Mg screw enhanced the expression of BMP-2 and VEGF at the tendon-bone interface and promoted the regeneration of fibrocartilaginous entheses.

3.4.9. In vivo fibrochondrogenesis induction assessment

The RT-qPCR analysis (Fig. 7d) revealed that the *in vivo* mRNA expression of fibrocartilage markers (Aggrecan, COL2A1 and SOX-9). The expression of fibrocartilage markers remained low in the early phase of tendon-bone healing, and greatly increased at 9 and 12 weeks ($p < 0.01$), indicating fibrochondrogenesis at the tendon-bone interface. Furthermore, the HP Mg group showed statistically higher expression of fibrocartilage markers than the Ti group at 9 and 12 weeks ($p > 0.05$). The changes in the fibrocartilage markers suggested the HP Mg screw was more effective in promoting fibrochondrogenesis, which was consistent with the relatively larger fibrocartilage area at the tendon-bone interface of the HP Mg group.

The GAG assay (Fig. 7e) showed that the level of the fibrocartilage matrix at the tendon-bone interface of the HP Mg group was significantly enhanced at 12 weeks in both groups ($p < 0.01$). The Ti group was comparatively lower in GAG production at 12 weeks postoperatively than the HP Mg group ($p < 0.01$), which was in consistence with the relatively small fibrocartilage area in the Ti group compared with the HP Mg group. Considering the western blot assay, RT-qPCR and GAG analysis at the tendon-bone interface, the HP Mg screw was more active in accumulating BMP-2 and VEGF at the tendon-bone interface in comparison with the traditional Ti metal. The BMP-2 and VEGF activated the expression of fibrocartilage markers (Aggrecan, COL2A1 and SOX-9) and production of fibrocartilage matrix (GAG) at the tendon-bone interface. And the highly differentiated fibrocartilage tissues marked the regeneration of fibrocartilaginous entheses.

4. Discussion

In the present study, we investigated the application of Mg interference screws in ACL reconstruction. The HP Mg screw provided rigid fixation of the tendon graft within the process of tendon-bone healing and demonstrated steady and uniform corrosion properties. The appropriate corrosion rate of the HP Mg screw matched the bony ingrowth rate in the bone tunnel with no bone tunnel enlargement or screw slip. The stable corrosion behaviour was partly due to the lack of impurities and the secondary phase [36,37]. In our previous study, the HP Mg orthopaedics screw also demonstrated uniform corrosion behaviour in fracture fixation [38].

Furthermore, the HP Mg screw promoted the regeneration of fibrocartilaginous entheses at the insertion site. Compared with the less differentiated fibrocartilage tissue in the Ti group, fibrocartilage transition zones between the tendon graft and bone were differentiated into uncalcified and calcified fibrocartilage tissues in the HP Mg group (Fig. 8a), similar to native fibrocartilaginous entheses in ACL, which contained four distinct transition zones in the sequence of ligament, uncalcified fibrocartilage, calcified fibrocartilage, and bone [39,40]. It is widely accepted that the long term goal of ACL reconstruction is to obtain biological incorporation of the graft at the anatomical attachment site of the ACL and to restore the transition from soft tissue to fibrocartilage, to calcified fibrocartilage, and to bone. The regeneration of fibrocartilaginous entheses in ACL construction was critical for graft stability and long-term clinical outcome. Although there was no significant difference between these two groups in aspects of the ROM and the biomechanical properties, the differentiation of the fibrocartilage interlayer into uncalcified and calcified regions had structure-functional significance in minimizing the stress concentration and transferring gradual load from soft tissue to bone and therefore enhanced the biological fixation of reconstructed ACL [41,42]. Moffat et al. [43] and Ferguson et al. [44] demonstrated that mineral presence in the mineralized fibrocartilage region led to increased compressive mechanical properties from uncalcified to calcified fibrocartilage regions. Therefore, the HP Mg screw enhanced the biological incorporation of the tendon graft at the insertion site and restored the gradual mechanical force transition.

During the corrosion of the HP Mg screw, high expression of BMP-2 and VEGF was detected both *in vitro* and *in vivo*. In comparison with the Ti extracts, the HP Mg extracts were effective in stimulating the expression of BMP-2 and VEGF and showed a significant difference at 7 days. The up-regulation of BMP-2 and VEGF was earlier than that of fibrocartilage markers, which occurred at 14 days. In the animal model, the Mg interference screw was superior to the Ti counterpart in stimulating BMP-2 and VEGF expression at the tendon-bone interface in the early phase of tendon-bone healing. Furthermore, BMPR1A, the specific receptor for BMP-2, was activated with the accumulation of BMP-2. The distribution and expression of BMPR1A at tendon-bone interface was relatively higher in HP Mg group in simultaneous comparison. These results indicated that the corrosion products of Mg devices might promote BMP-2 and VEGF expression in tendon-bone healing. In a previous report, Li et al. [45] observed an increase in BMP-2 expression in hBMSCs after culturing in pure Mg and Mg alloy extracts. Yoshizawa et al. [25] demonstrated the enhancement of VEGF expression and extracellular matrix production in undifferentiated hBMSCs cultured in medium containing 20 mM $MgSO_4$. Guo et al. [24] implanted Mg alloy AZ31 into the femoral periosteum of a rat

represents fibrocartilage, UFC represents uncalcified fibrocartilage, CFC represents calcified fibrocartilage) (b) Histological scores of the tendon-bone interface in ACL reconstruction. (c) Calculated fibrocartilage area at the tendon-bone interface. Semi-quantitative scores of (d) BMP-2, (e) VEGF and (f) BMPR1A immunohistochemical staining at the tendon-bone interface. * denotes $p < 0.05$; ** denotes $p < 0.01$; ▲ denotes $p < 0.05$ compared with the HP Mg extract group; ▲▲ denotes $p < 0.01$ compared with the HP Mg extract group.

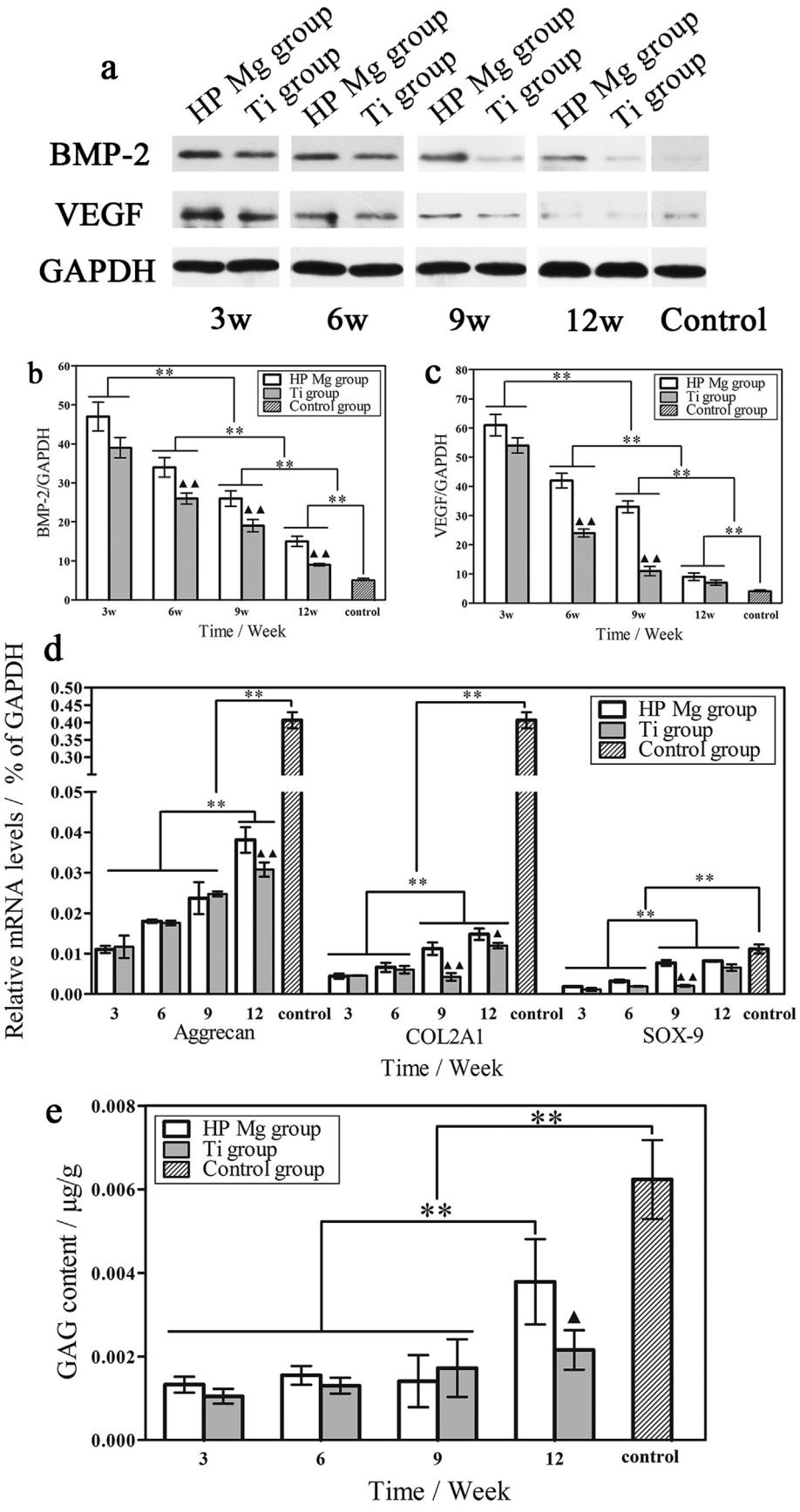

Fig. 7. (a) Western blot assay of BMP-2 and VEGF expression in tissues at the insertion site of the tendon graft and native ACL 3, 6, 9 and 12 weeks after surgery. Densitometry of BMP-2 (b) and VEGF (c) in the western blot assay. Gene expression of fibrocartilage markers (Aggrecan, COL2A1, SOX-9) (d) and GAG production (e) of the tendon graft 3, 6, 9 and 12 weeks after surgery. * denotes $p < 0.05$; ** denotes $p < 0.01$; ▲ denotes $p < 0.05$ compared with the HP Mg group; ▲▲ denotes $p < 0.01$ compared with the HP Mg group.

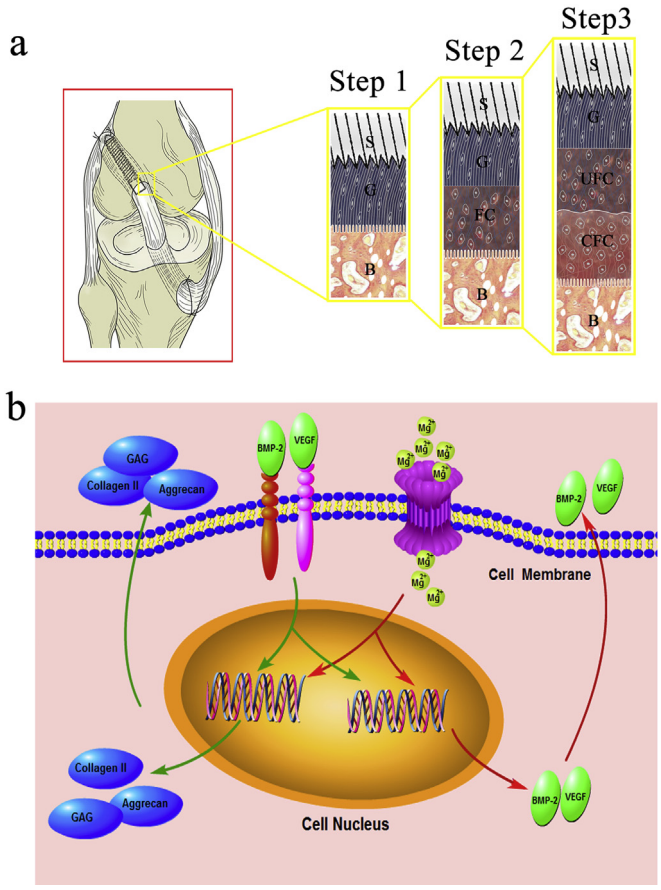

Fig. 8. Schematic diagrams show the mechanism of the Mg interference screw stimulating fibrocartilaginous entheses regeneration. (a) Semitendinosus autograft fixed by the Mg interference screw to the femoral tunnel and the regeneration process of the fibrocartilaginous entheses at the entrance of the femoral tunnel (Step 1–Step 3). At the interlayer between the tendon graft (G) and bone (B), which was fixed by Mg interference screw (S) (Step1), the fibrocartilage layer (FC) formed at the tendon-bone interface (Step2) and was further dived into uncalcified fibrocartilage (UFC) and calcified fibrocartilage (CFC) layers (Step 3). (b) Mg^{2+} was released from the HP Mg screw. The Mg^{2+} went through the ion channel and up-regulated BMP-2 and VEGF expression. Excreted BMP-2 and VEGF then activated intracellular signalling pathways and stimulated the synthesis of the fibrocartilage matrix (Collagen II, Aggrecan and GAG) with the assistance of Mg^{2+}.

model and observed high expression of BMP-2 in the surrounding bone tissues. Thus, Mg ions released from Mg devices might be responsible for BMP-2 and VEGF accumulation.

Although the mechanism of fibrocartilaginous entheses regeneration is not fully understood, the promoting effect of growth factors (BMP-2 and VEGF) is widely accepted. BMP-2 is critical in tendon-bone junction development and fibrocartilage entheses formation [21,46,47]. Hashimoto et al. [46] injected recombinant human bone morphogenetic protein-2 (rhBMP-2) into the flexor digitorum communis tendon of a rabbit hind limb and found that fibrocartilaginous entheses formed one month after the transfer of the tendon-bone complex onto the surface of the rabbit tibia. Kim et al. [47] filled the anchor hole in a rabbit patellar tendon model with 1 μg BMP-2 and observed an organized fibrocartilage layer at the tendon-bone interface in the histological analysis compared with the group not treated with BMP-2. VEGF can stimulate up-regulation of BMP-2 [19] and promote capillary permeability and angiogenesis in ACL reconstruction via vascular endothelial cells [23,48]. In the present study, there was apparent accumulation of BMP-2 and VEGF in the early phase of tendon-bone healing according to immunohistochemical analysis and western blot assay. The *in vitro* studies showed that the accumulation of BMP-2 and VEGF was responsible for up-regulation of fibrocartilage markers (Aggrecan, COL2A1 and SOX-9) and fibrocartilage matrix (GAG). In this way, BMP-2 and VEGF stimulated fibrochondrogenesis and promoted the regeneration of fibrocartilaginous entheses at the tendon-bone interface.

Therefore, Mg promoted fibrocartilaginous entheses regeneration in signal pathways involving BMP-2 and VEGF. As depicted in Fig. 8b, Mg ions released from corroded HP Mg screws and stimulated the expression and secretion of BMP-2 and VEGF. Extracellular BMP-2 and VEGF in accumulation up-regulated the expression of fibrocartilage markers (Aggrecan, COL2A1 and SOX-9) and initiated synthesis of the fibrocartilage matrix (Collagen II, Aggrecan and GAG) via receptor binding to pluripotent stem cells. In the process of tendon-bone healing, newly formed fibrocartilage matrix at the tendon-bone interface gradually formed a fibrocartilage layer and further differentiated into uncalcified and calcified fibrocartilage layers. The highly specialized tendon-bone interface was consistent with native ACL entheses, indicating the regeneration of fibrocartilaginous entheses in ACL reconstruction.

5. Conclusions

HP Mg was investigated as biodegradable materials of interference screw in the rabbit model of ACL reconstruction for its potential in fibrocartilaginous entheses regeneration.

(1) The extracts of HP Mg screws enhanced cell viability of hBMSCs *in vitro*. Compared with the extracts of the Ti screw, the HP Mg extracts promoted the expression of BMP-2 and VEGF at 7 days, increased fibrocartilage markers (Aggrecan, COL2A1 and SOX-9) and enhanced GAG production after 14 days of culturing.
(2) In the animal model of ACL reconstruction, the HP Mg screw demonstrated steady and uniform corrosion *in vivo* with no signs of infection, deformity, dislocation or severe host reaction. All rabbits obtained morphological and functional recovery, and the biomechanical properties of the reconstructed ACL in HP Mg group were comparable to the Ti group. Most importantly, the HP Mg group performed mature fibrocartilaginous entheses with the highly specialized transition zone at the tendon-bone interface 12 weeks after surgery, compared with the less organized fibrocartilage tissues in the Ti group.
(3) The mechanism of Mg interference screw promoting fibrocartilaginous entheses regeneration was via BMP-2 and VEGF accumulation. In cell experiment, the HP Mg extracts promoted significantly higher expression of BMP-2 and VEGF in hBMSCs than the Ti extracts, and led to enhanced expression of fibrocartilage markers (Aggrecan, COL2A1 and SOX-9) and production of GAG. In the animal model, the Mg interference screw was superior to the Ti counterpart in stimulating BMP-2 and VEGF expression at the tendon-bone interface in the early phase of tendon-bone healing. The accumulation of BMP-2 and VEGF at the tendon-bone interface promoted the regeneration of fibrocartilaginous transition zones between the tendon graft and the bone, which showed promise for the clinical use of biodegradable Mg interference screw in tendon graft fixation and biological attachment reconstruction.

Acknowledgements

This work was supported by the Natural Science Foundation of China (No. 51271117, 81371935), the Biomedical Program of Science and Technology innovation project supported by Shanghai (No.

14441901801, No. 14441901802), and the National Basic Research Program of China (973 Program, No. 2012CB619102). The author, Shaoxiang Zhang, gratefully acknowledges the support of the Jiangsu Nature Science Foundation for Young Scholars (No. BK2012206).

References

[1] K. Hayashi, T. Kumai, I. Higashiyama, Y. Shinohara, T. Matsuda, Y. Takakura, Repair process after fibrocartilaginous enthesis drilling: histological study in a rabbit model, J. Orthop. Sci. Off. J. Jpn. Orthop. Assoc. 14 (2009) 76–84.
[2] R.R. Cooper, S. Misol, Tendon and ligament insertion. A light and electron microscopic study, J. Bone Jt. Surg. Am. Vol. 52 (1970) 1–20.
[3] C.C. Prodromos, Y. Han, J. Rogowski, B. Joyce, K. Shi, A meta-analysis of the incidence of anterior cruciate ligament tears as a function of gender, sport, and a knee injury-reduction regimen, Arthrosc. J. Arthrosc. Relat. Surg. Off. Publ. Arthrosc. Assoc. N. Am. Int. Arthrosc. Assoc. 23 (2007), 1320.e6–1325.e6.
[4] G.R. Barrett, F.K. Noojin, C.W. Hartzog, C.R. Nash, Reconstruction of the anterior cruciate ligament in females: a comparison of hamstring versus patellar tendon autograft, Arthrosc. J. Arthrosc. Relat. Surg. Off. Publ. Arthrosc. Assoc. N. Am. Int. Arthrosc. Assoc. 18 (2002) 46–54.
[5] D.C. Fithian, E.W. Paxton, M.L. Stone, W.F. Luetzow, R.P. Csintalan, D. Phelan, et al., Prospective trial of a treatment algorithm for the management of the anterior cruciate ligament-injured knee, Am. J. Sports Med. 33 (2005) 335–346.
[6] D.N. Caborn, M. Coen, R. Neef, D. Hamilton, J. Nyland, D.L. Johnson, Quadrupled semitendinosus-gracilis autograft fixation in the femoral tunnel: a comparison between a metal and a bioabsorbable interference screw, Arthrosc. J. Arthrosc. Relat. Surg. Off. Publ. Arthrosc. Assoc. N. Am. Int. Arthrosc. Assoc. 14 (1998) 241–245.
[7] W. Singhatat, K.W. Lawhorn, S.M. Howell, M.L. Hull, How four weeks of implantation affect the strength and stiffness of a tendon graft in a bone tunnel: a study of two fixation devices in an extraarticular model in ovine, Am. J. Sports Med. 30 (2002) 506–513.
[8] B.L. Shafer, P.T. Simonian, Broken poly-L-lactic acid interference screw after ligament reconstruction, Arthrosc. J. Arthrosc. Relat. Surg. Off. Publ. Arthrosc. Assoc. N. Am. Int. Arthrosc. Assoc. 18 (2002) E35.
[9] A. Werner, A. Wild, A. Ilg, R. Krauspe, Secondary intra-articular dislocation of a broken bioabsorbable interference screw after anterior cruciate ligament reconstruction, Knee Surg. Sports Traumatol. Arthrosc. Off. J. ESSKA 10 (2002) 30–32.
[10] M.H. Baums, B.A. Zelle, W. Schultz, T. Ernstberger, H.M. Klinger, Intraarticular migration of a broken biodegradable interference screw after anterior cruciate ligament reconstruction, Knee Surg. Sports Traumatol. Arthrosc. Off. J. ESSKA 14 (2006) 865–868.
[11] F.A. Krappel, E. Bauer, U. Harland, The migration of a BioScrew as a differential diagnosis of knee pain, locking after ACL reconstruction: a report of two cases, Arch. Orthop. Trauma Surg. 126 (2006) 615–620.
[12] C.M. Hettrich, S. Gasinu, B.S. Beamer, M. Stasiak, A. Fox, P. Birmingham, et al., The effect of mechanical load on tendon-to-bone healing in a rat model, Am. J. Sports Med. 42 (2014) 1233–1241.
[13] C.M. Hettrich, S.A. Rodeo, J.A. Hannafin, J. Ehteshami, B.E. Shubin Stein, The effect of muscle paralysis using Botox on the healing of tendon to bone in a rat model, J. Shoulder Elb. Surg. Am. Shoulder Elb. Surg. [et al] 20 (2011) 688–697.
[14] Y.F. Zheng, X.N. Gu, F. Witte, Biodegradable metals, Mater. Sci. Eng. R Rep. 77 (2014) 1–34.
[15] K.F. Farraro, K.E. Kim, S.L.Y. Woo, J.R. Flowers, M.B. McCullough, Revolutionizing orthopaedic biomaterials: the potential of biodegradable and bioresorbable magnesium-based materials for functional tissue engineering, J. Biomech. 47 (2014) 1979–1986.
[16] C.K. Hagandora, M.A. Tudares, A.J. Almarza, The effect of magnesium ion concentration on the fibrocartilage regeneration potential of goat costal chondrocytes, Ann. Biomed. Eng. 40 (2012) 688–696.
[17] F. Feyerabend, F. Witte, M. Kammal, R. Willumeit, Unphysiologically high magnesium concentrations support chondrocyte proliferation and redifferentiation, Tissue Eng. 12 (2006) 3545–3556.
[18] Y. Dou, N. Li, Y. Zheng, Z. Ge, Effects of fluctuant magnesium concentration on phenotype of the primary chondrocytes, J. Biomed. Mater. Res. Part A 102 (2014) 4455–4463.
[19] S.A. Rodeo, Biologic augmentation of rotator cuff tendon repair, J. Shoulder Elb. Surg. Am. Shoulder Elb. Surg. [et al] 16 (2007) S191–S197.
[20] G.M. Kuang, W.P. Yau, W.W. Lu, K.Y. Chiu, Osteointegration of soft tissue grafts within the bone tunnels in anterior cruciate ligament reconstruction can be enhanced, Knee Surg. Sports Traumatol. Arthroscopy Off. J. ESSKA 18 (2010) 1038–1051.
[21] L. Obert, D. Lepage, F. Gindraux, P. Garbuio, Bone morphogenetic proteins in soft-tissue reconstruction, Injury 40 (Suppl. 3) (2009) S17–S20.
[22] W. Friess, H. Uludag, S. Foskett, R. Biron, Bone regeneration with recombinant human bone morphogenetic protein-2 (rhBMP-2) using absorbable collagen sponges (ACS): influence of processing on ACS characteristics and formulation, Pharm. Dev. Technol. 4 (1999) 387–396.
[23] N. Ferrara, Vascular endothelial growth factor: basic science and clinical progress, Endocr. Rev. 25 (2004) 581–611.
[24] Y. Guo, L. Ren, C. Liu, Y. Yuan, X. Lin, L. Tan, et al., Effect of implantation of biodegradable magnesium alloy on BMP-2 expression in bone of ovariectomized osteoporosis rats, Mater. Sci. Eng. C Mater. Biol. Appl. 33 (2013) 4470–4474.
[25] S. Yoshizawa, A. Brown, A. Barchowsky, C. Sfeir, Magnesium ion stimulation of bone marrow stromal cells enhances osteogenic activity, simulating the effect of magnesium alloy degradation, Acta Biomater. 10 (2014) 2834–2842.
[26] H. Sun, C. Wu, K. Dai, J. Chang, T. Tang, Proliferation and osteoblastic differentiation of human bone marrow-derived stromal cells on akermanite-bioactive ceramics, Biomaterials 27 (2006) 5651–5657.
[27] J.P. Spalazzi, M.C. Vyner, M.T. Jacobs, K.L. Moffat, H.H. Lu, Mechanoactive scaffold induces tendon remodeling and expression of fibrocartilage markers, Clin. Orthop. Relat. Res. 466 (2008) 1938–1948.
[28] C.H. Chang, C.H. Chen, H.W. Liu, S.W. Whu, S.H. Chen, C.L. Tsai, et al., Bioengineered periosteal progenitor cell sheets to enhance tendon-bone healing in a bone tunnel, Biomed. J. 35 (2012) 473–480.
[29] M.P. van den Borne, N.J. Raijmakers, J. Vanlauwe, J. Victor, S.N. de Jong, J. Bellemans, et al., International Cartilage Repair Society (ICRS) and Oswestry macroscopic cartilage evaluation scores validated for use in autologous chondrocyte implantation (ACI) and microfracture, Osteoarthr. Cartil. OARS Osteoarthr. Res. Soc. 15 (2007) 1397–1402.
[30] C.Y. Wen, L. Qin, K.M. Lee, K.M. Chan, Peri-graft bone mass and connectivity as predictors for the strength of tendon-to-bone attachment after anterior cruciate ligament reconstruction, Bone 45 (2009) 545–552.
[31] N. Erdmann, N. Angrisani, J. Reifenrath, A. Lucas, F. Thorey, D. Bormann, et al., Biomechanical testing and degradation analysis of MgCa0.8 alloy screws: a comparative in vivo study in rabbits, Acta Biomater. 7 (2011) 1421–1428.
[32] G.M. Kuang, W.P. Yau, W.W. Lu, K.Y. Chiu, Use of a strontium-enriched calcium phosphate cement in accelerating the healing of soft-tissue tendon graft within the bone tunnel in a rabbit model of anterior cruciate ligament reconstruction, Bone Jt. J. 95-B (2013) 923–928.
[33] A. Bedi, D. Kovacevic, C. Hettrich, L.V. Gulotta, J.R. Ehteshami, R.F. Warren, et al., The effect of matrix metalloproteinase inhibition on tendon-to-bone healing in a rotator cuff repair model, J. Shoulder Elb. Surg. Am. Shoulder Elb. Surg. [et al] 19 (2010) 384–391.
[34] Y. Kadonishi, M. Deie, T. Takata, M. Ochi, Acceleration of tendon-bone healing in anterior cruciate ligament reconstruction using an enamel matrix derivative in a rat model, J. Bone Jt. Surg. Br. Vol. 94 (2012) 205–209.
[35] V. Lovric, M. Ledger, J. Goldberg, W. Harper, N. Bertollo, M.H. Pelletier, et al., The effects of low-intensity pulsed ultrasound on tendon-bone healing in a transosseous-equivalent sheep rotator cuff model, Knee Surg. Sports Traumatol. Arthrosc. Off. J. ESSKA 21 (2013) 466–475.
[36] R. Walter, M.B. Kannan, A mechanistic in vitro study of the microgalvanic degradation of secondary phase particles in magnesium alloys, J. Biomed. Mater. Res. Part A 103 (2015) 990–1000.
[37] N.I. Zainal Abidin, B. Rolfe, H. Owen, J. Malisano, D. Martin, J. Hofstetter, et al., The in vivo and in vitro corrosion of high-purity magnesium and magnesium alloys WZ21 and AZ91, Corros. Sci. 75 (2013) 354–366.
[38] P. Han, P. Cheng, S. Zhang, C. Zhao, J. Ni, Y. Zhang, et al., In vitro andin vivo studies on the degradation of high-purity Mg (99.99wt.%) screw with femoral intracondylar fractured rabbit model, Biomaterials 64 (2015) 57–69.
[39] A.S. Panni, G. Milano, L. Lucania, C. Fabbriciani, Graft healing after anterior cruciate ligament reconstruction in rabbits, Clin. Orthop. Relat. Res. (1997) 203–212.
[40] R. Newsham-West, H. Nicholson, M. Walton, P. Milburn, Long-term morphology of a healing bone-tendon interface: a histological observation in the sheep model, J. Anat. 210 (2007) 318–327.
[41] S.A. Rodeo, S.P. Arnoczky, P.A. Torzilli, C. Hidaka, R.F. Warren, Tendon-healing in a bone tunnel. A biomechanical and histological study in the dog, J. Bone Jt. Surg. Am. Vol. 75 (1993) 1795–1803.
[42] M. Kurosaka, S. Yoshiya, J.T. Andrish, A biomechanical comparison of different surgical techniques of graft fixation in anterior cruciate ligament reconstruction, Am. J. Sports Med. 15 (1987) 225–229.
[43] K.L. Moffat, W.H. Sun, P.E. Pena, N.O. Chahine, S.B. Doty, G.A. Ateshian, et al., Characterization of the structure-function relationship at the ligament-to-bone interface, Proc. Natl. Acad. Sci. U. S. A. 105 (2008) 7947–7952.
[44] V.L. Ferguson, A.J. Bushby, A. Boyde, Nanomechanical properties and mineral concentration in articular calcified cartilage and subchondral bone, J. Anat. 203 (2003) 191–202.
[45] R.W. Li, N.T. Kirkland, J. Truong, J. Wang, P.N. Smith, N. Birbilis, et al., The influence of biodegradable magnesium alloys on the osteogenic differentiation of human mesenchymal stem cells, J. Biomed. Mater. Res. Part A 102 (2014) 4346–4357.
[46] Y. Hashimoto, G. Yoshida, H. Toyoda, K. Takaoka, Generation of tendon-to-bone interface “enthesis” with use of recombinant BMP-2 in a rabbit model, J. Orthop. Res. Off. Publ. Orthop. Res. Soc. 25 (2007) 1415–1424.
[47] J.G. Kim, H.J. Kim, S.E. Kim, J.H. Bae, Y.J. Ko, J.H. Park, Enhancement of tendon-bone healing with the use of bone morphogenetic protein-2 inserted into the suture anchor hole in a rabbit patellar tendon model, Cytotherapy 16 (2014) 857–867.
[48] T. Yoshikawa, H. Tohyama, H. Enomoto, H. Matsumoto, Y. Toyama, K. Yasuda, Expression of vascular endothelial growth factor and angiogenesis in patellar tendon grafts in the early phase after anterior cruciate ligament reconstruction, Knee Surg. Sports Traumatol. Arthrosc. Off. J. ESSKA 14 (2006) 804–810.